Downselection and Basic Properties of Additively Manufactured ODS Alloys

T. S. Byun
D. A. Collins
K. B. Fillingim
T. A. Feldhausen
H. C. Hyer
Y. R. Lin
D. T. Hoelzer
K. O. Hanson

August 2023

M3CT-23OR1304061

DOCUMENT AVAILABILITY

Reports produced after January 1, 1996, are generally available free via OSTI.GOV.

> ***Website*** www.osti.gov

Reports produced before January 1, 1996, may be purchased by members of the public from the following source:

> National Technical Information Service
> 5285 Port Royal Road
> Springfield, VA 22161
> ***Telephone*** 703-605-6000 (1-800-553-6847)
> ***TDD*** 703-487-4639
> ***Fax*** 703-605-6900
> ***E-mail*** info@ntis.gov
> ***Website*** http://classic.ntis.gov/

Reports are available to US Department of Energy (DOE) employees, DOE contractors, Energy Technology Data Exchange representatives, and International Nuclear Information System representatives from the following source:

> Office of Scientific and Technical Information
> PO Box 62
> Oak Ridge, TN 37831
> ***Telephone*** 865-576-8401
> ***Fax*** 865-576-5728
> ***E-mail*** reports@osti.gov
> ***Website*** https://www.osti.gov/

Advanced Materials and Manufacturing Technologies Program

DOWNSELECTION AND BASIC PROPERTIES OF ADDITIVELY MANUFACTURED ODS ALLOYS

T. S. Byun
D. A. Collins
K. B. Fillingim
T. A. Feldhausen
H. C. Hyer
Y. R. Lin
D. T. Hoelzer
K. O. Hanson

August 2023

M3CT-23OR1304061

CONTENTS

LIST OF FIGURES

LIST OF TABLES

ACKNOWLEDGEMENTS

DOWNSELECTION AND BASIC PROPERTIES OF ADDITIVELY MANUFACTURED ODS ALLOYS

ABSTRACT

In the Advanced Materials and Manufacturing Technologies (AMMT) program, the work package for development of new materials aimed to explore the advanced manufacturing techniques that are feasible for the manufacturing of advanced materials components. A merit-based feasibility study was attempted to identify an accelerated development path for oxide dispersion strengthened (ODS) alloys by creatively combining additive manufacturing (AM) technologies with the recent advances in ODS materials and traditional manufacturing technologies. For FY 2023, the primary tasks were to develop AM and post-build processing routes for ODS ferritic (Fe-Cr alloy or 14YWT) and austenitic (Fe-Cr-Ni alloys or 316L and 316H) alloys and to perform basic microstructural and mechanical characterizations to provide feedback to the alloy and processing design. Furthermore, the multi-laboratory effort collaboratively created a decision criteria matrix to evaluate and downselect the new materials processed by advanced manufacturing methods. This report describes the ODS alloy processing routes combining AM processes and post-build thermomechanical treatments, mechanical and microstructural characteristics of the newly developed materials, and the application results of the decision criteria matrix for the additively manufactured ODS alloys, including a downselected material and feasible processing route. Key mechanical test results, including tensile strength, tensile ductility, and fracture toughness data, are reported, and explained. Higher strength was measured from the ferritic ODS alloys, whereas higher ductility and fracture toughness were measured from the austenitic ODS alloys. Many of the decision criteria were scored the same for the additively manufactured ferritic and austenitic ODS alloys; however, the austenitic alloys generally have higher corrosion resistance and significantly better ductility. Although these scores are not significantly different to make them highly discernable, the austenitic ODS alloys were downselected to be the primary materials group in the future research on ODS materials in the AMMT program.

1. INTRODUCTION

The structural materials used in advanced nuclear reactors designed for high thermal and economic efficiencies will be subject to high-temperature, high-dose neutron irradiations. Exposing a material to such extreme conditions will significantly modify the material's microstructure and local chemistry and thus degrade its mechanical, chemical, and physical properties [1]. Therefore, the reactor core components for any high-performance reactor will require excellent high-temperature mechanical properties, high radiation resistance, and high corrosion resistance, in addition to a feasible manufacturing process. Design and selection of key structural materials for such high-performance reactors will require considerable research on feasible manufacturing routes and significantly enhanced materials property databases.

To achieve the required reactor materials performance—in particular, high thermal and radiation resistances—the candidate metallic alloys are typically processed to have the fine-grained microstructures that can be stabilized using various strong and thermally stable nanoparticles, such as oxides, carbides, and nitrides [1, 2, 3, 4, 5, 6, 7]. In the past two decades, highly stable nanoparticles such as fine oxides or oxygen-enriched nanoclusters have become the most important constituent in the future fission and fusion reactor materials. For example, the 14YWT nanostructured ferritic alloy (NFA) is an advanced ODS ferritic alloy that can deliver excellent high-temperature strength and creep properties as well as high radiation tolerance because of its unique microstructure of ultrasmall grains and high concentration (~[5–10] $\times 10^{23}$ m^{-3}) of nanoscale (~2–5 nm) Ti-Y-O–rich nanoclusters [8, 9]. The nanoclusters show

remarkable high-temperature stability: up to about 1,400°C for short times and at about 825°C for around 7 years in creep testing [10, 11]. The large interfacial area associated with these microstructural features provides the high point-defect sink strength that is beneficial to radiation tolerance. Results of recent ion irradiation studies show that the 14YWT alloy has the lowest void swelling for doses up to 500 dpa in the temperature range 400°C–500°C compared with various steels and other ODS alloys [12]. Several helium-ion irradiation studies have also demonstrated that these microstructures trap helium atoms and form high-density nanoscale bubbles rather than coarse bubbles at grain boundaries.

Despite all the advances established for the 14YWT NFA and its variants, so far, the only viable processing path for producing the advanced ODS alloys is high-energy mechanical alloying, which involves a week or days of high-energy ball milling a gas-atomized alloy powder with a small quantity (~0.3 wt.%) of yttria (Y_2O_3) powder followed by an extrusion path to produce solid products. The Ti-Y-O–rich nanoparticles precipitate during this consolidation process. However, using this processing route might have prohibitively high cost for mass production of any component, and the long process route is not practical for commercial applications. Without a breakthrough innovation to resolve this issue, the enormous merits of the distribution of highly stable nanoparticles in metallic materials will be missing in the future of advanced reactor technologies. Lately, the AM method based on laser melting was proposed as an alternative manufacturing route for the ODS alloys. This AM method is feasible for producing ODS alloys because the local cooling rate after the laser melting is so high that some oxygen content can be retained in a solid-solution state and later can be precipitated into oxide particles in a controlled thermomechanical condition.

AM technologies can provide many opportunities and challenges if they are used to build a nuclear reactor structure. These technologies offer enormous flexibility in designing and building complex components that can be cost prohibitive with traditional manufacturing methods. Indeed, recent research efforts confirmed that the austenitic steels are highly suitable for AM of complex shaped reactor components [13, 14, 15]. This suitability likely comes from the fast cooling that occurs during the AM process, preventing the formation of the high-temperature ferrite (i.e., δ-ferrite) phase in austenitic steels during cooling. Phase decomposition and segregation occurring in this metastable phase cause degradation at high temperatures. Examples of key AM technologies that might be relevant to manufacturing of nuclear reactor structures include the laser powder bed fusion (LPBF) and laser-directed energy deposition (DED) methods. In principle, the microstructures—and thus the mechanical properties—of additively manufactured alloys can be tailored by changing the processing parameters, such as scan speed, laser power, powder feedstock purity, and powder layer thickness [16, 17, 18]. In particular, the size and orientation of the fine-grained dislocation cell structure in metallic materials can be controlled by changing processing parameters [19, 20, 21] or applying post-build heat treatments [17].

Although an optimized LPBF process can produce a very fine and desirable metastable microstructure owing to the fast cooling and solidification, many unknowns and adverse effects remain regarding the microstructural and chemical stability of additively manufactured materials in high-temperature, corrosion, and irradiation environments. The as-printed materials usually display increased room temperature yield strength (YS) but less work hardening because of the characteristic microstructure of fine grains and dislocation cells formed during the localized rapid solidification [19, 22, 23, 24]. Recent test results indicate that these fine-grained structures with mobile dislocations can shorten the high-temperature creep life [13, 14, 20]. Furthermore, the fracture toughness of additively manufactured materials could be reduced by the increased porosity from the build process, structural anisotropy relative to the build direction, and inclusions from impurities in the feedstock powder [15, 25]. Neutron or ion irradiation could also significantly affect the behaviors (i.e., shortened creep life and reduced fracture toughness) observed in additively manufactured alloys [15, 26, 27, 28]. Some of these property degradation mechanisms can be more pronounced in ferritic alloys and ferritic–martensitic steels [29, 30]. The ferritic alloys usually have relatively lower initial ductility compared with the austenitic alloys, and

2

therefore the reduction of ductility owing to any causes mentioned above can significantly embrittle the alloy. Furthermore, the complex but often incomplete phase transformations that occur during the repeated reheating of deposited layers can make the microstructural evolution of the ferritic or ferritic-martensitic steels significantly more complex compared with other single-phase alloy systems such as the nickel-based alloys [29, 30].

Because the combination of some embrittling features from AM processing—such as the high porosity, incomplete transformation (residual δ-ferrite), and metastable state with high residual stress—can result in significantly degraded properties, the manufacturing process for reactor components may require a post-build process to obtain a high-performance alloy. This post-build process may include a controlled thermomechanical treatment (TMT). Therefore, the AM-based production of a component will require a processing route that combines multiple materials processing methods. This research project focuses on understanding potential candidate ODS alloys and on downselecting specific alloys and processing routes that would provide significant benefit when fabricated using advanced manufacturing technologies.

The AMMT program has an overarching goal to accelerate the development, evaluation/qualification, and deployment of advanced materials by employing advanced manufacturing technologies to enable reliable and economical nuclear energy technologies. To achieve the common goal, this research pursued accelerated approaches to develop and understand potential candidate alloys and to downselect a specific material and feasible processing route. The accelerated approach also harnesses existing knowledge for the candidate materials and feasible manufacturing technologies in the decision-making process by incorporating a selection criteria matrix.

For FY 2023, the research tasks have focused on developing an AM and post-build processing route for ODS nuclear materials and to perform microstructural and mechanical characterizations to provide feedback to the materials and processing route design. Furthermore, Oak Ridge National Laboratory (ORNL) collaborated with Los Alamos National Laboratory (LANL) and Pacific Northwest National Laboratory (PNNL), to develop a common decision criteria matrix to prioritize new materials produced via the combined manufacturing processes. The items comprising the matrix include, but are not limited to, neutronic performance, fabricability, ability to withstand corrosive/extreme environments, high-temperature mechanical properties, oxidation/steam resistance, thermal management ability, and coating adhesion. This report describes the ODS alloy processing routes combining AM processes and post-build TMTs, mechanical and microstructural characteristics of the newly developed materials, and the application results of the decision criteria matrix for the AM ODS alloys—a downselected material and feasible processing route.

2. MATERIALS AND MECHANICAL TESTING

2.1 Production of Ferritic ODS materials

In production of ferritic ODS alloys, the high-chromium ferritic alloy 14YWT powder from ORNL inventory was used. The 14YWT powder was a pre-alloyed powder with nominal composition of Fe-14Cr-3W-0.4Ti (wt %) and a nominal powder size of about 44 µm produced by argon gas atomization at Allegheny Technologies Incorporated. To introduce nano-oxide particles in the material, an additional oxygen source was needed for the alloy powder. The 14YWT powder was mixed with oxide powders (Y_2O_3 and Fe_2O_3) to three different combinations: 0.3 wt % Y_2O_3 was added to all three mixtures, and different amounts of Fe_2O_3 powder (0, 0.1, and 0.3 wt %) were added to the 14YWT alloy powder–Y_2O_3 mixture to compensate for the loss of oxygen content in processing and the inefficient nonuniform distribution of oxygen within the materials.

3

The DED method was used to consolidate the powder mixtures. The local melting and rapid cooling nature of the DED additive process is used as a rapid solidification–cooling method that is needed to produce a microstructure without overgrown oxide particles. Some key processing parameters (after optimization) include a stepover size of 2 mm, a layer height of 0.75 mm, a laser spot size of 2.5 mm, a power of 1,020 W, a beam feed rate of 750 mm/min, and a powder flow rate of 5.4 g/min. Under these conditions, twenty-nine mini-blocks of ~38 mm × 12.7 mm × 12.7 mm were produced for three powder mixtures.

The final step of the production process was controlled hot-rolling. Part of the mini-blocks were hot-rolled after annealing at 700°C or 800°C for 10 min. These annealing temperatures were chosen for processing because limited coarsening of the steel microstructures, including oxide particles, was expected. This TMT consisted of multiple annealing–rolling steps, and the final thickness of the rolled coupons was about 5 mm, which introduced a heavy deformation of about 60% to the alloys. These rolled coupons were sent to machine shop to extract miniature tensile and fracture specimens. The face-normal directions of these specimens coincide with the build direction in the AM process and with the thickness-reduction direction in hot-rolling. The materials with three different oxide additions and in three different TMT conditions make nine different materials in total. Table 1 summarizes the mixtures, AM processes, and TMP conditions.

Table 1. Materials and processing of additively manufactured ferritic ODS steels

Material ID	Composition	AM method	TMT condition
AM-YY	Fe-14Cr-3W-0.4Ti-0.3Y_2O_3	DED	None
AM-YY-700	Fe-14Cr-3W-0.4Ti-0.3Y_2O_3	DED	Hot-rolling at 700°C for 60% reduction
AM-YY-800	Fe-14Cr-3W-0.4Ti-0.3Y_2O_3	DED	Hot-rolling at 800°C for 60% reduction
AM-YYF	Fe-14Cr-3W-0.4Ti-0.3Y_2O_3-0.1Fe_2O_3	DED	None
AM-YYF-700	Fe-14Cr-3W-0.4Ti-0.3Y_2O_3-0.1Fe_2O_3	DED	Hot-rolling at 700°C for 60% reduction
AM-YYF-800	Fe-14Cr-3W-0.4Ti-0.3Y_2O_3-0.1Fe_2O_3	DED	Hot-rolling at 800°C for 60% reduction
AM-YF	Fe-14Cr-3W-0.4Ti-0.3Y_2O_3-0.3Fe_2O_3	DED	None
AM-YF-700	Fe-14Cr-3W-0.4Ti-0.3Y_2O_3-0.3Fe_2O_3	DED	Hot-rolling at 700°C for 60% reduction
AM-YF-800	Fe-14Cr-3W-0.4Ti-0.3Y_2O_3-0.3Fe_2O_3	DED	Hot-rolling at 800°C for 60% reduction

Figure 1. ODS alloy coupons (about 1 in. wide) after DED and TMT processes.

2.2   Production of Austenitic ODS materials

Two austenitic alloy powders were the base materials the production of ODS alloys: 316L and 316H powders. These powders have chemistries within the standard composition ranges: Fe-(16–18)Cr-(10–14)Ni-(2–3)Mo-0.03(max)C and Fe-(16–18)Cr-(10–14)Ni-(2–3)Mo-(0.04–0.1)C, respectively. These alloy powders were both produced by argon gas atomization and 15–45 μm powder feedstock from Praxair. The Y_2O_3 powder was added to the alloy powders and thoroughly mixed to introduce oxygen content and/or nano-oxide particles in the AM process. The optimum or typical amount of Y_2O_3 added to the ODS base alloys is about 0.3 wt.%. Part of the oxygen source is expected to be lost in the nanoparticle formation process because the oxygen distribution after AM is highly inhomogeneous. To compensate for this loss to inefficient microstructure sites, an amount higher than the optimum content, 0.5 wt %, was added to the two austenitic alloys. The high ductility of the austenitic stainless-steel matrix can accommodate this higher oxide amount while retaining enough ductility for structural applications.

The LPBF method was used to consolidate these austenitic alloy powder–oxide powder mixtures. The mixed SS316L+yttria and SS316H+yttria powders were processed using a Renishaw AM250 LPBF system. The AM250 is equipped with a 400 W, ytterbium-fiber pulsed laser with a spot size of about 70 μm and wavelength of 1.07 μm. Six 62 mm wide, 37 mm high, 12 mm thick plates were printed for the two powder mixtures using the following parameters: a laser power of 225 W, point distance of 65 μm, exposure time of 105 μs, hatch spacing of 100 μm, and a layer thickness of 50 μm. A standard stripe pattern linear hatch scan strategy was adopted: a stripe width of 5 mm and a scan rotation of 67° between consecutive layers. All builds were performed at room temperature in an inert argon atmosphere, keeping the O_2 level below 500 ppm, and using a mild steel build plate. These plates were cut into 14–17 mm high bars for convenient thermomechanical processes.

In the same way as the processing for ferritic ODS alloys, the final step of the production process involved controlled hot-rolling steps. The bars were thermomechanically processed (repeatedly hot-rolled) with annealing at 700°C or 800°C for 10 min. The rolling consisted of multiple annealing–rolling steps, and the final thickness of the rolled coupons was about 5 mm. This height reduction corresponds to a plastic strain of 70%. Miniature tensile and fracture specimens were machined from these coupons. The face-normal directions of these specimens coincide with the build direction in the AM processes, which is the same as the thickness-reduction direction in hot-rolling. The two alloys in three different TMT conditions make six different materials in total, as summarized in Table 2.

Table 2. Materials and processing of additively manufactured austenitic ODS steels

Material ID	Composition	AM method	TMT condition
AM-316L	316L	LPBF	None
AM-316L-700	316L	LPBF	Hot-rolling at 700°C for 70% reduction
AM-316L-800	316L	LPBF	Hot-rolling at 800°C for 70% reduction
AM-316H	316H	LPBF	None
AM-316H-700	316H	LPBF	Hot-rolling at 700°C for 70% reduction
AM-316H-800	316H	LPBF	Hot-rolling at 800°C for 70% reduction

Figure 2. ODS alloy coupons (about 1 in. wide) after LPBF and TMT processes.

2.3 Mechanical Property Evaluation of Newly Produced Alloys

Two types of mechanical testing specimens were machined for property evaluations. The first type was the SS-J2 tensile specimen, which has a 1.2 mm wide, 0. 5 mm thick, and 5 mm long gage section; a total length of 16 mm; and a head width of 4 mm. The second type was a miniature fracture bend bar side-grooved (MBS) that can be precracked and fracture-tested under three-point bend (TPB) loading mode. It is a rectangular bar with nominal dimensions of 14 mm length × 4 mm width × 2.5 mm thickness. At the middle of the bar, a 1 mm deep electrical discharge machined notch is introduced, and 20%-deep grooves are machined at both sides of the specimen.
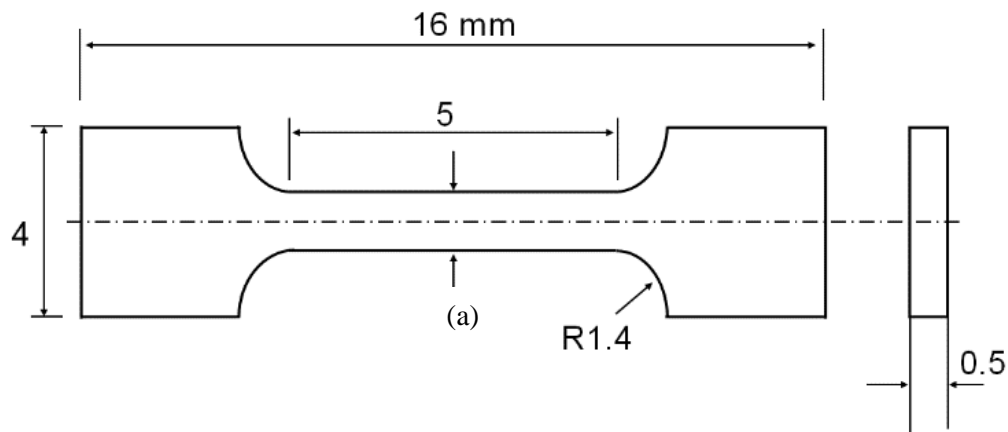
Figure 3. Miniature mechanical testing specimen designs: (a) SS-J2 tensile specimen and (b) three-point bend bar specimen.
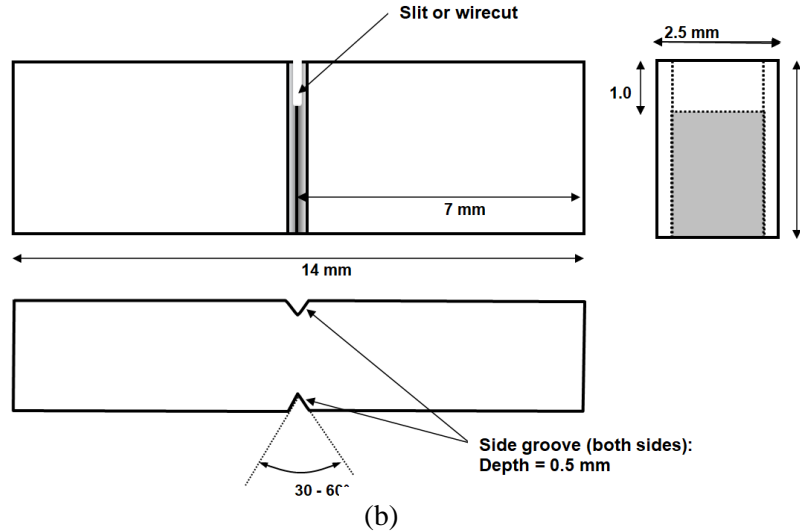
Figure 4 (continued). Miniature mechanical testing specimen designs:(a) SS-J2 tensile specimen and (b) three-point bend bar specimen.

Uniaxial tensile testing for SS-J2 specimens was performed by using an electromagnetic mechanical testing system at a nominal strain rate of 1×10^{-3} s^{-1} (displacement rate = 0.3 mm/min) by using shoulder-loading grip sets [30]. The loading direction coincided with the rolling direction. Raw data or load-displacement data up to failure were recorded and used to determine the common engineering strength and ductility parameters, including YS, ultimate tensile strength (UTS), uniform elongation (UE), and total elongation (TE). Unless specified otherwise, tensile testing and data analysis were performed by following the standard testing procedure in ASTM E8/8M and E21.

Fracture toughness testing in TPB mode was also performed using the electromagnetic mechanical testing system. The span of the TPB loading was 12.5 mm. A streamlined procedure from precracking to static fracture testing to fracture toughness calculation, which was established for miniature fracture testing by the lead author [6, 5, 31], was applied to the fracture toughness testing of the 14 mm long miniature specimens. The omission of the externally attached clip gage for displacement measurements and the use of the self-guiding, cradle-type specimen grip both enabled high-efficiency processing in this project. A simplified fracture resistance (J-integral) vs. crack growth resistance (J-R) curve calculation procedure was established by adopting the load-displacement curve normalization method with a slight modification that separates the displacement measurements into elastic and plastic components.

Before the static fracture (J-R) testing, every single-edged MBS specimen was fatigue-precracked to create a sharp crack tip extending from the 1 mm deep machined notch. The ferritic specimens were loaded cyclically from 200 or 250 N maximum to 50 N minimum at 10 Hz, and the austenitic specimens were loaded from 600 N maximum to 50 N minimum at 15 Hz. After allowing the samples to "settle" for about 1,000 cycles, the peak displacement value was recorded, and the test machine was programmed to terminate precracking once the peak displacement increased by 15 μm. Next, the crack was sharpened by loading at half the initial amplitude while maintaining the 50 N minimum for an additional 10,000 cycles. The result was a sharp fatigue precrack with an approximately 1.8 mm total depth, or 45% the specimen thickness. Creating a sharp crack in front of the notch tip is required to conduct a static fracture toughness test to evaluate fracture resistance and critical stress intensity (K) values. The static fracture tests were performed in compressive bend loading mode at a displacement speed of about 0.005 mm/s (0.3 mm/min). Monotonic load vs. displacement data were recorded at a typical data acquisition rate of 5 Hz

during the static testing. These data were used to generate J-R curves and determine fracture toughness values (J_Q and K_{JQ}). The J-R curves were constructed from the load-displacement curve data and optical measurements of the crack lengths using the curve normalization method, which was modified in this case for the miniature specimens.

Except for a few special techniques used for the miniature specimen, the fracture testing and calculation practices used in the project followed the ASTM Standard Test Methods E1820 and E399. The following special techniques were used. (1) The testing does not use any attached gage for displacement measurement. To calculate the load-displacement curve, the linear displacement component, including pure elastic displacement and machine load-line compliance, was removed, and the elastic displacement was reconstructed using the theoretical equation. (2) An iterative calculation method was used to meet the final crack length physically measured, which is an ultimate criterion defined in the curve normalization method. (3) Precracking was based on the reading of displacement amplitude only. Fatigue cracking length was considered achieved when the displacement amplitude changed by a defined amount under a given load amplitude.

Only part of the tensile and fracture testing campaign has been completed, along with the thorough microscopy analysis. Therefore, much of the scoring process in the decision-making or downselecting on materials discussed in Section 4 relied on the existing knowledge and some conjectures from the limited newly measured mechanical property or known data for similar ODS materials. Testing for high-temperature properties and microscopy examinations will be continued.

3. MECHANICAL PROPERTIES

The test results for the newly produced additively manufactured ferritic and austenitic ODS alloys are summarized in the following subsections and are used in later sessions as the input for mechanical properties to apply the decision criteria for the downselection of the AM ODS materials. In the following subsections, the engineering strength parameters (YS and UTS) and ductility parameters (UE and TE) are presented and compared among the processing routes. Fracture toughness data are also presented for the ferritic ODS alloys. These comparisons may lead to the downselection of a more feasible alloy and processing route within the ODS materials. Mechanical testing in the higher temperature range up to 600°C is underway.

3.1 Mechanical Properties of Ferritic ODS materials

The YS and UTS data for the ferritic ODS alloys are compared in Figure 5, which displays the strength data of nine different materials conditions. Because the ferritic ODS alloys exhibit YS typically about 800 MPa, which is about twice that of non-ODS ferritic–martensitic alloys (400–500 MPa), the value can be a criterion for screening processing routes.

Notably, the AM-YF material ($14YWT+0.3Y_2O_3+0.3F_2O_3$) in all three conditions (as-built condition and after 700°C and 800°C TMT) exhibits both YS and UTS higher than 800 MPa. The AM-YY material ($14YWT+0.3Y_2O_3$) also displays decent strength in the as-built condition, but the strength in the 700°C TMT condition only exhibits high enough strength for the criterion. The AM-YYF material ($14YWT+0.3Y_2O_3+0.1F_2O_3$) in all conditions exhibits strengths less than 800 MPa. These strength data indicate that the amount of oxygen in the powder mixture matters, and the precipitation of oxide particles is incomplete in the AM and subsequent TMP process.

8
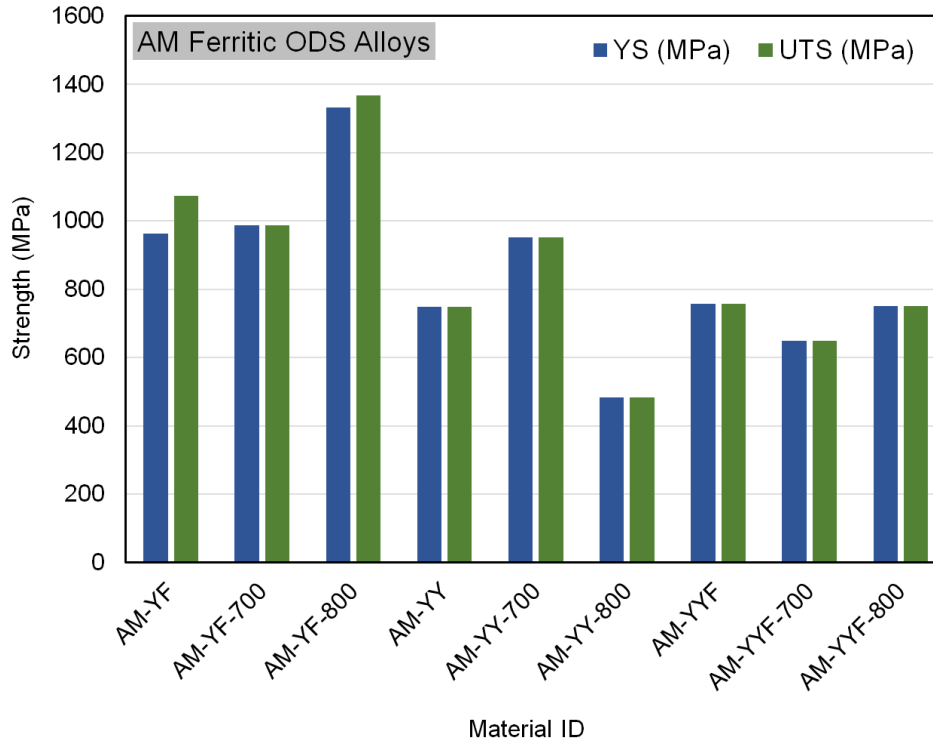
Figure 5. Tensile strength of additively manufactured ferritic ODS alloys.

The ductility data (UE and TE) display much simpler comparison, Figure 6, because many of the ferritic ODS alloys produced for this research exhibit embrittlement or zero ductility. The AM-YF in the as-built condition demonstrates a significant ductility for such a high-strength (~1 GPa) material. Both UE and TE are about 5% and achieving the 5% UE is a particularly meaningful result for the strength level. The same alloy after the 800°C TMT also displays some ductility, but its limited ductility might originate from small inelastic deformation around the yield strain range, which is often observed in near-embrittled materials. Therefore, these comparisons of the strength and ductility parameters among the processing routes and oxide contents made it obvious that the AM-YF ferritic ODS is the most feasible for an acceptable mechanical function as a structural material.

Figure 7 compares the fracture toughness data (in MPa√m unit) of AM ferritic ODS materials. All nine different fratcure toughness values are within a relatively narrow range of 18–33 MPa√m. These relatively low fracture toughness values indicate that the test temperature (room temperature) is near the lower tail of the brittle-to-ductile transition range. The upper-shelf fracture toughness of ferritic ODS alloys is typically higher than 100 MPa√m. Demonstrating a proper level of fracture toughness (>100 MPa√m) is essential to a structural material for thick component applications. A structural material with fracture toughness less than 100 MPa√m may not show stable crack growth at high tempeatures. Therefore, the application of the ferritic ODS alloys as presented should be limited to the components requiring high strength only.
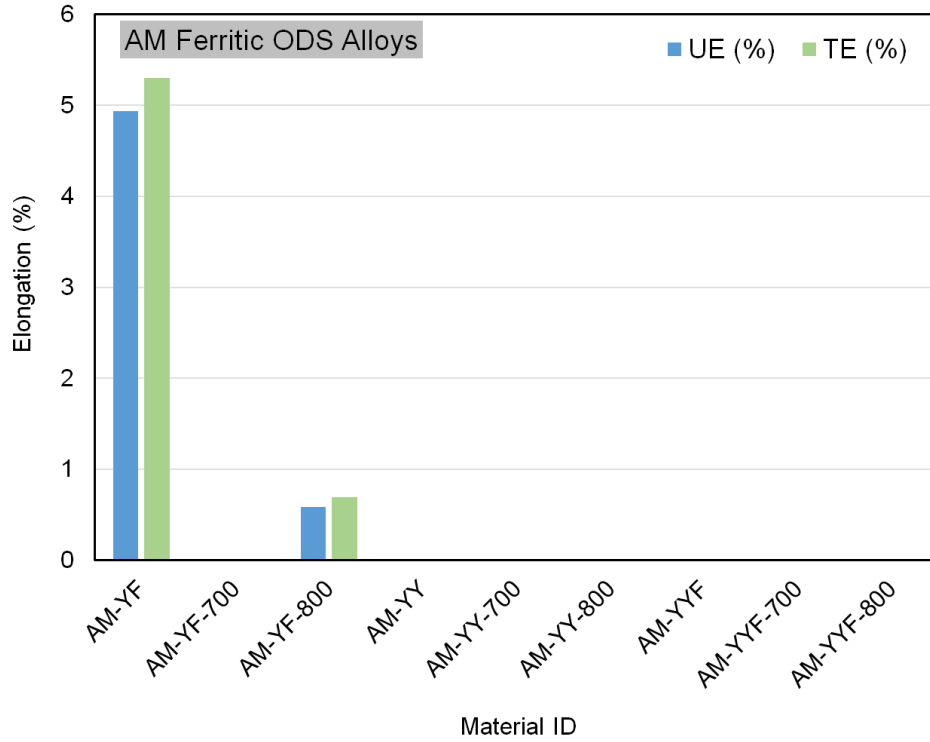
Figure 6. Tensile ductility of additively manufactured ferritic ODS alloys (with nil-ductility of embrittled materials).
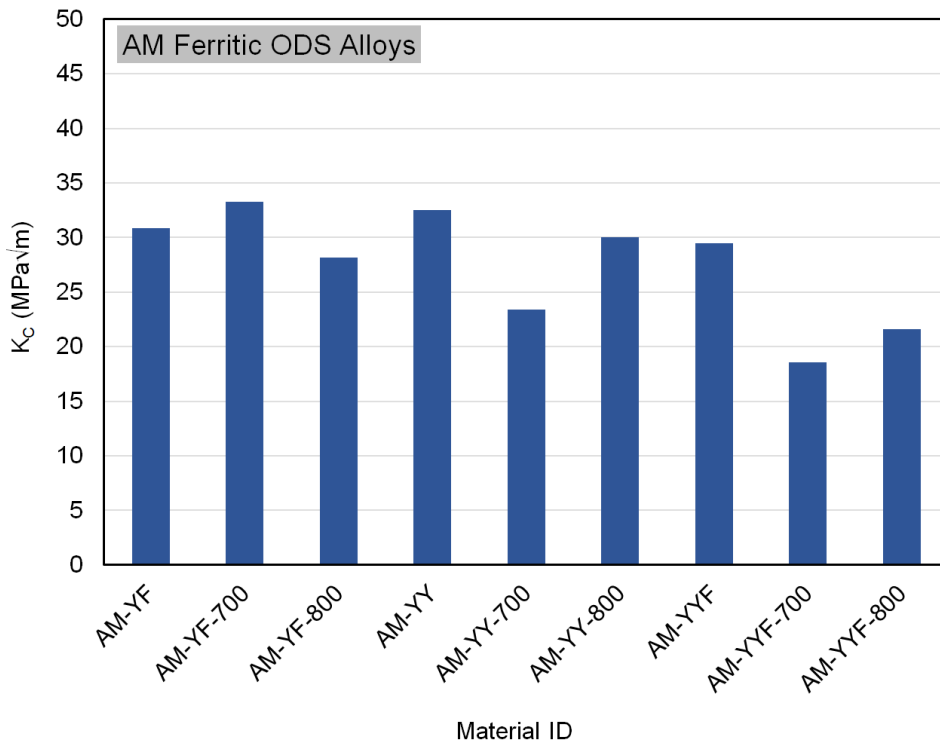
Figure 7. Fracture toughness (K_C) of additively manufactured ferritic ODS alloys.

3.2 Mechanical Properties of Austenitic ODS materials

The tensile test results for the two austenitic ODS (316L and 316H) alloys are presented in Figure 8 and Figure 9, respectively, for their room temperature strength and ductility data. Compared with the test results for the ferritic ODS alloys, the strength of additively manufactured austenitic ODS alloys is generally lower, but their ductility is much higher. Overall, these austenic ODS alloys are more feasible for the engineering applications requiring high mechanical saftey margins.
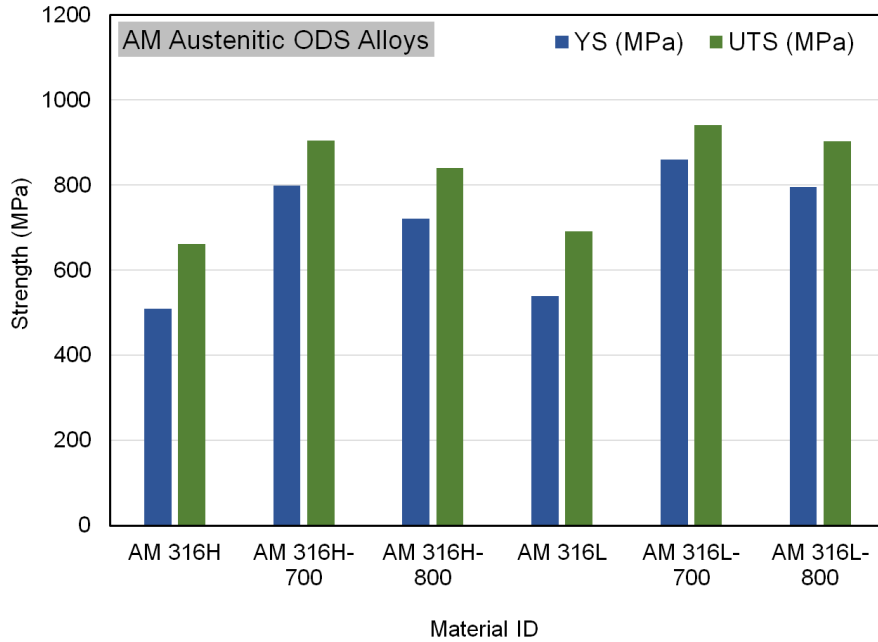
Figure 8. Tensile strength of additively manufactured austenitic ODS alloys.
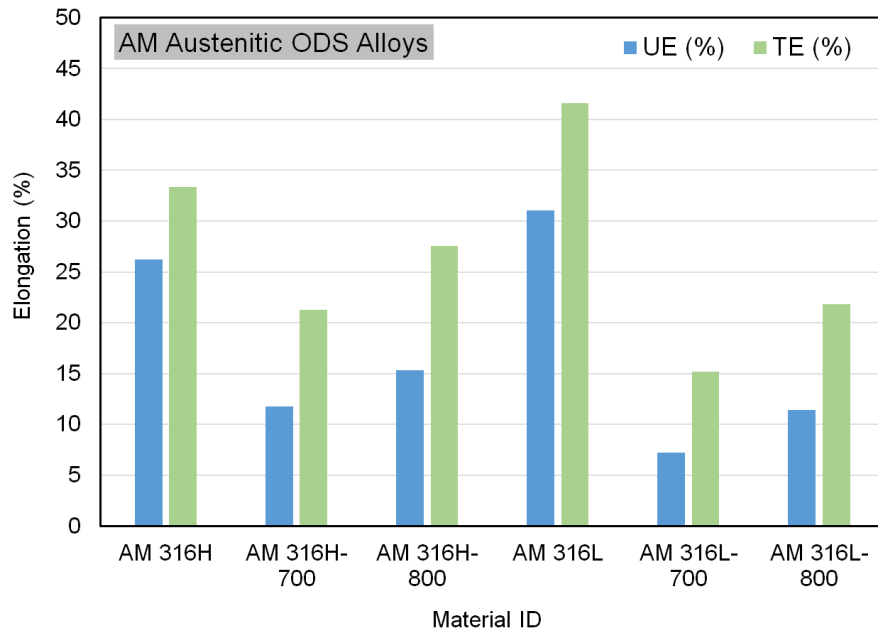
Figure 9. Tensile ductility of additively manufactured austenitic ODS alloys.

11

If the same strength criterion of 800 MPa is applied, then the AM 316L-700 is the only material that satisfies the criterion, as seen in Figure 8. The AM 316H-700 and AM 316L-800 nearly meet the criterion because their YS valus are slighly lower than 800 MPa, but their UTS values are above 900 MPa. Considering that the wrought 316L and 316H steels in the annealed condition have YS and UTS of about 200 MPa and about 500 MPa, respectively, the strengths of these additively manufactured ODS variants of the same alloys are remarkable. Meanwhile, the as-built ODS materials, with material IDs AM 316L and AM 316H, also exhibit much higher strengths comapred with the wrought materials. However, their strengths are only slightly (20%–30%) higher than those of the AM 316L without oxide strengthening.

The strength of 316H with a higher carbon content (typically within 0.04–0.1 wt %) is slighty lower than that of 316L with a limited amount of carbon content (<0.03 wt %) in all processing conditions. Such a small difference in strength might not significantly affect other mechanical behavior; however, the role of carbon content in strengthening the additively manufactured materials should be a fundamental topic to explore.

Figure 9 compares the ductility data of the additively manufactured austenitic ODS alloys. First of all, the ODS 316L in the as-built condition demonstrates the highest ductility among the materials tested: UE is higher than 30%, and TE is higher than 40%. The ODS 316H in the as-built condition exhibits the next highest ductility. The AM ODS alloys after 700°C and 800°C TMTs have relatively lower ductilities as the strength of those increased by the TMTs. Overall, the ductility of the additively manufactured austenitic ODS alloys is significant (all UE > 6%), and no embrittlement is observed within the material conditions tested.

Another notable aspect observed is the size of necking ductility (TE-UE). Significant necking ductility is important because it is a key element to prevent any catastroscopic crack growth in any structure under loading. A minimum of 7% necking ductility was observed in the additively manufactured austenitic ODS steels tested.

Figure 10 presents the fracture toughness data of additively manufactured austenitic ODS materials. The as-printed 316L alloy demonstrats an outstanding fracture toughness at 227 MPa√m, whereas the fratcure toughness of all others is much lower and within a narrow range of 130–170 MPa√m. In the 316L alloy, both of the post-build treatments reduced fracture toughness to the same degree. This result is different from the behavior of the 316H alloy that exhibits slight increases in fracture toughness from 156 MPa√m, much lower than 227 MPa√m, after the same post-build treatments. Although the fracture toughness measurements, except for that of the as-printed ODS 316L alloy, are not considered high enough for the structures under high stress, no materials show any evidence of embrittlement, and these ODS materials with fracture toughness values above 100 MPa√m are considered feasible for general structural applications. Furthermore, these fracture toughness data indicate that the test temperature (room temperature) is in the upper-shelf range or near upper-shelf range of the temperature transition curve of the materials. Therefore, compared with the ferritic ODS materials, the application of the austenitic ODS alloys processed via AM and post-build TMT can be much more feasible in various conditions.
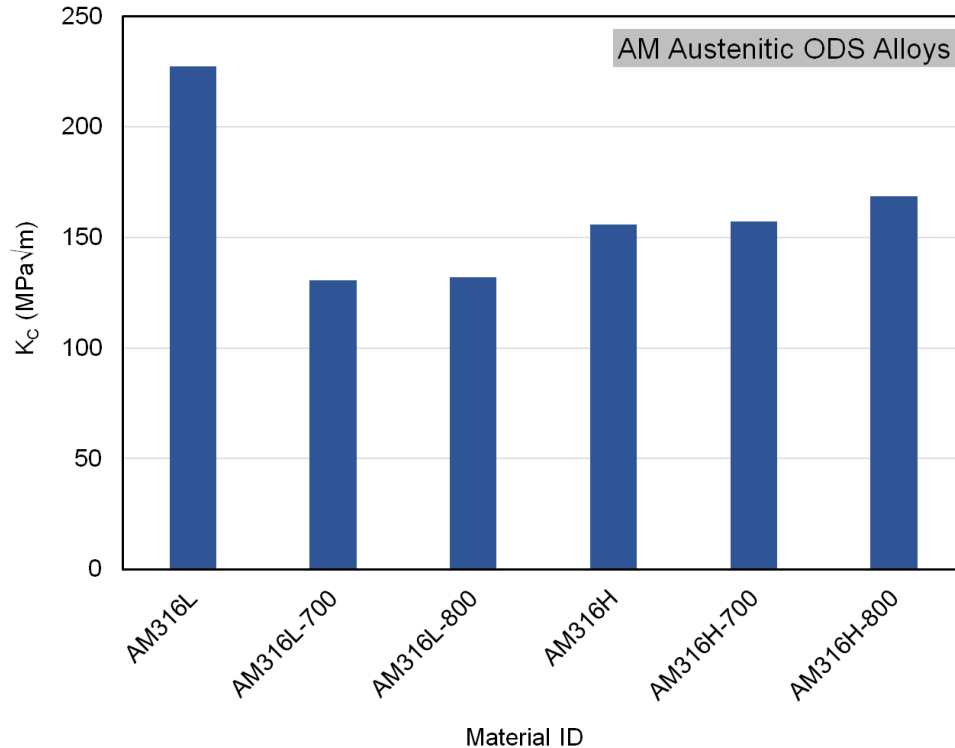
Figure 10. Fracture toughness (K$_C$) of additively manufactured austenitic ODS alloys.

4. DECISION CRITERIA MATRIX AND MATERIALS DOWNSELECTION

4.1 Decision Criteria Matrix

Structural materials for nuclear applications are exposed to various extreme conditions. Many variables can arise from the combination of different materials, manufacturing routes, properties, and service environments, thereby complicating the materials assessment process. The AMMT program focuses mostly on the materials that must be produced by advanced or nontraditional processing methods. In this research, these materials are categorized as new materials because their mechanical, physical, and chemical properties are different from their variants produced by traditional processing routes, which typically consist of melting, solidification, and TMTs. The assessment of these new materials will require an evaluation instrument with a set of systematic scoring criteria [32] to objectively evaluate the suitability and maturity of the new materials for nuclear applications.

ORNL, LANL and PNNL collaborated to develop a common decision criteria matrix for the prioritization of new materials produced via various and combined advanced manufacturing processes. The scoring items comprising the matrix include, but are not limited to, neutronic performance, fabricability, ability to withstand corrosive/extreme environments, high-temperature mechanical properties, oxidation/steam resistance, thermal management ability, and coating adhesion. These items were categorized into four property criteria groups: application space, environmental compatibility, physical and mechanical properties, and manufacturability.

The scores, ranging from 1 (poor) to 5 (excellent), were also established to consider a variety of aspects of new materials, with agreement among the participants. Applying these criteria primarily allows for

reasonable evaluation of new materials based on the limited accumulation of property data and knowledge. The result can be used for preliminary downselection of materials and processing methods. The main conclusion from the application of the criteria matrix is a recommendation on the downselected ODS materials and their feasible processing routes. Table 3 through Table 6 summarize the product of the multi-laboratory collaborative work: the decision criteria matrix for downselecting the new materials.

Table 3. Decision criteria matrix and scoring criteria for the application space of new materials

Category	Criteria	Evaluation	Score Reference				
			5	4	3	2	1
Application Space	Applicability to Different Reactor Types	Can the material be used in multiple reactor types or is it only suitable for a few?	Potential application for material across all Generation IV reactor types.	Potential application for material in 4 to 5 of the Generation IV reactor types.	Potential application for material in 2 to 3 of the Generation IV reactor types.	Potential application of material in only one reactor type.	No conceivable application for material in any reactor type.
	Other Industry Experience	Do other industries use this material and/or are other industries interested in this material?	Widespread use of this material in multiple industries.	Material is used extensively in only a few other industries but has widespread interest in other industries.	Material has only moderate use and interest in other industries.	The material has limited use and interest in other industries.	Other industries do not use or have any interest in the material.
	Data Availability	The availability and comprehensiveness of data associated with a given material.	Material has been extensively studied for use in nuclear energy and data is published and available.	One or two notable gaps exist in data, otherwise material has been studied and data is published and available.	Several studies have been performed on material and data is available, but there are still several notable gaps in data.	Relatively few studies have been performed on material with limited published data.	Limited or no information or data available for specified material.
	Code & Standards Availability	The availability of codes and standards which govern the production, material quality/standards, and implementation of a material.	Codes and Standards are available for the material, its production, and its most likely application.	Codes or standards are available for 4-5 of the areas.	Codes or standards are only available for 3 of the areas.	Codes or standards are only available for 2 of the areas	Codes and standards are only available for ≤1 area.
	Component Versatility	The potential for a material to be used for different types of components.	Material has potential for application in all types of components.	Material has potential for application in 3/4 types of components.	Material has potential for application in 2/4 types of components.	Material has potential for application in 1/4 types of components.	Material does not have potential for application in any type of components.

Table 4. Decision criteria matrix and scoring criteria for the environmental compatibility of new materials

Category	Criteria	Evaluation	Score Reference				
			5	4	3	2	1
Environmental Compatibility	**Radiation Resistance**	The ability of a material to maintain its shape, size, and properties after exposure to radiation.	Material exhibits <1% volumetric change and limited mechanical property degradation at doses of ≥300 dpa	Material exhibits <1% volumetric change and limited mechanical property degradation at doses between 200-300 dpa	Material exhibits <1% volumetric change mechanical property degradation at doses between 100-200 dpa	Material exhibits <1% volumetric change and limited mechanical property degradation at doses between 50-100 dpa	Material exhibits <1% volumetric change and limited mechanical property degradation at doses ≤50 dpa
	Elemental Transmutation	Elemental stability of a material and impact of transmutation.	Transmutation of elements in the material is not a concern.	Transmutation of elements in the material results in at least one of the concerns or only causes concern when dose received is comparable to the reactor or material lifetime. Meaning the material would be replaced before transmutation was cause for concern.	Transmutation of elements in the material results in two of the concerns, or transmutation is only a concern in one neutron spectrum (either fast or thermal) but not the other.	Transmutation of the elements in the material leads to premature material failure or three of the major concerns.	Transmutation of constituent elements disqualifies the material from consideration or results in all of the major concerns.
	High Temperature Oxidation Resistance	The ability of a material to resist oxidation at high temperatures.	Oxidation initiation occurs at temperatures ≥ 800°C	Oxidation initiation occurs at temperatures ≥ 600°C	Oxidation initiation occurs at temperatures ≥ 400°C	Oxidation initiation occurs at temperatures ≥ 200°C	Oxidation initiation occurs at temperatures < 200°C
	Neutronics Compatibility	Degree of negative impact to the neutron economy of reactors.	Material has a low thermal and fast neutron capture cross section and exhibits no detrimental reactions to either spectrum of neutrons.	Material has moderately low thermal or fast neutron capture cross sections.	Material has a low neutron capture cross section in one of either thermal or fast spectrums.	Material has moderately high thermal or fast neutron capture cross sections, making it likely unsuitable for in-core applications.	Material is a known neutron absorber, or has a large neutron capture cross section at both fast and thermal energies.
	Coolant Compatibility & Corrosion Resistance	# of coolants, corrosion, erosion considerations The material's relative stability in a given coolant, including its resistance to corrosion, erosion, and other chemical reactions.	Material is compatible with all types of coolants, showing no significant degradation.	Material is compatible with 3/4 types of coolants, exhibiting good stability and inertness.	Material is compatible with two types of coolants, exhibiting good stability in those coolants.	Material is compatible in only one type of coolant, exhibiting significant instability in the other types of coolants.	Material is not compatible with any of the coolant types, showing significant degradation in short periods of time.

Table 5. Materials scoring criteria for the physical and mechanical properties of new materials.

Category	Criteria	Evaluation	Score Reference				
			5	4	3	2	1
Physical & Mechanical Properties	Thermal Conductivity	Capability (with high thermal conductivity) to increase the thermal efficiency of an energy system and reduce transitional thermal stress in the components.	Maintain > 100 W/mK over lifetime.	Maintain 50 - 100 W/m.K over lifetime.	Maintain 10 - 50 W/m.K over lifetime.	Falls to < 10 W/m.K in the end of lifetime.	Begins with a low thermal conductivity < 10 W/m.K.
	Thermal Capacity	General thermal capacity such as melting point, softening point, phase stability across temperature range.	Operation temperatures in all reactor types < 0.4 TM	Operation temperatures in most reactor types in 0.4–0.6 TM	Operation temperatures in some reactor types in 0.4–0.6 TM	Operation temperatures in some reactor types > 0.6 TM	Operation temperatures in most reactor types > 0.6 TM
	Tensile Properties	High temperature tensile properties including strength, ductility, and type of failure	Yield strength > 200 MPa; uniform ductility > 2%; no brittle failure mode over lifetime	Yield strength > 150 MPa; uniform ductility > 2%; no brittle failure mode over lifetime	Yield strength > 100 MPa; uniform ductility > 2%; no brittle failure mode over lifetime	Yield strength > 100 MPa; uniform ductility > 2%; possibly brittle failure mode in lifetime	Yield strength > 100 MPa; uniform ductility < 2%; possibly brittle failure mode in lifetime
	Creep Performance	Risk of losing dimension stability in long-term service	No creep rupture expected in lifetime. No measurable creep strain (<0.001% in lifetime) in all reactor types	No creep rupture expected in lifetime. Little creep strain < 0.01 % in lifetime in most reactor types.	No creep rupture expected in lifetime. No creep strain < 0.1 % in lifetime in most reactor types.	No creep rupture expected in lifetime. Creep strain > 0.1 % in lifetime in some reactor types.	Possible creep rupture in lifetime. Creep strain > 1 % in lifetime in some reactor types.
	Fatigue	Risk of component failure due to crack growth by cyclic loading	Load conditions in most reactor types are more than 20% below the fatigue limit.	Load conditions in some reactor types are more than 20% below the fatigue limit.	Load conditions in most reactor types are close but below the fatigue limit.	Load conditions in some reactor types are above the fatigue limit.	Load conditions in most reactor types are above the fatigue limit.
	Fracture Toughness	Capability to avoid the most probable failure mode with aging and degradation	Fracture toughness > 150 MPa√m over lifetime.	Fracture toughness > 100 MPa√m over lifetime.	Fracture toughness > 50 MPa√m over lifetime.	Fracture toughness > 50 MPa√m over most of lifetime.	Fracture toughness < 50 MPa√m over most of lifetime.
	Microstructural Dependency	The sensitivity of material's properties to its microstructure	Properties are not sensitive to microstructure and processing route. Microstructure is highly stable in any service environment.	Properties are not sensitive to microstructure and processing route. Microstructure is reasonably stable in most of service environments.	Properties are somewhat dependent on microstructure and processing route. Microstructure is reasonably stable in most of service environments.	Properties are sensitive to microstructure and processing route. Microstructure is reasonably stable in most of service environments.	Properties are sensitive to microstructure and processing route. Microstructure is not stable in some service environments.
	Scope for Microstructural Enhancement	The possibility of enhancing material properties by microstructural engineering through feasible processing routes	Microstructure is easily controlled for desirable properties within traditional and advanced processing means. No limitation in mass production and product size.	Microstructure is easily controlled for desirable properties within traditional and advanced processing means. Some limitations in mass production and product size.	Microstructure can be controlled for desirable properties through a few limited processing methods only.	Microstructure can be controlled for desirable properties through a specially designed processing method only.	Microstructure can be controlled for a few properties through a specially designed processing method only.

17

Table 6. Materials scoring criteria for the manufacturability of new materials

Category	Criteria	Evaluation	Score Reference				
			5	4	3	2	1
Manufacturability	Reproducibility/ Consistency	Degree of reproducibility and consistency in product quality for various manufacturing routes/methods of the same material (e.g., For the same material, 3D printing is not consistent, but casting is)	Number of critical parameters that need to be carefully monitored >1	Number of critical parameters that need to be carefully monitored >3	Number of critical parameters that need to be carefully monitored >5	Number of critical parameters that need to be carefully monitored >7	Number of critical parameters that need to be carefully monitored >9
	Process Complexity	# of processing steps (when writing, provide post processing information)	If it involves: 0 preprocessing steps but a maximum of 1 post processing steps	If it involves:0-1 preprocessing steps but a maximum of 2 post processing steps	If it involves: 0-2 preprocessing steps but a maximum of 3 post processing steps	If it involves: 0-3 preprocessing steps but a maximum of 4 post processing steps	If it involves: 0-4 preprocessing steps but a maximum of 5 post processing step
	Cost	Overall cost for production of components (considering the same concern as Reproducibility/Consistency)	If it the overall cost is 30-50% lower than the current commercial processing method	If the overall cost is 10-30% lower than the current commercial processing method	If the overall cost is comparable to the current commercial processing method	If the overall cost is 10-30% higher than the current commercial processing method	If the overall cost is 30-50% higher than the current commercial processing method
	Scalability	The ability to increase the overall # of components being produced with a certain material, and the ability to produce dimensionally larger components	Zero concerns in terms of time delay/additional required equipment/ for scaling up	1-3 concerns in terms of time delay/additional required equipment/ for scaling up	3-5 concerns in terms of time delay/additional required equipment/ for scaling up	5-7 concerns in terms of time delay/additional required equipment/ for scaling up	Almost impossible to scale up
	Production Method Technological Readiness Level (TRL)	The already qualified processing techniques receive a score of 5 and the ones still in the process a 3 and completely new processes receive 1	The processes with TRL between 7 and 9	The processes with TRL between 5 and 7	The processes with TRL between 3 and 5	The processes with TRL between 1 and 3	First report on the process
	Raw Material Supply	Precursor availability in the United States	If all the raw materials required for the process are manufactured and supplied in the U.S. Also, the supplier/manufacturer is cheapest among the available sources internationally.	If all the raw materials required for the process are manufactured and supplied in the U.S. Also, the supplier/manufacturer is not cheapest among the available sources internationally.	If all the raw materials required for the process are not manufactured in the U.S. but the supplier is based in the U.S.	If all the raw materials required for the process are not manufactured in the U.S but can be shipped internationally	If all the raw materials required for the process are not manufactured in the U.S but cannot be shipped internationally

Table 6 (continued). Materials scoring criteria for the manufacturability of new materials

Category	Criteria	Evaluation	Score Reference				
			5	4	3	2	1
Manufacturability	**Flexibility of Manufacturing**	# of methods which can be used to manufacture material	if the material can be manufactured via 100% of the available processing techniques	If the material can be manufactured via 80% of the available processing techniques	If the material can be manufactured via 60% of the available processing techniques	If the material can be manufactured via 40% of the available processing techniques	If the material can be manufactured via 20% of the available processing techniques
	Conventional Machining	Need for drilling, joining, welding, riveting etc.	A ready-to-go part can be directly manufactured without any post-processing	A ready-to-go part can be directly manufactured with negligible post-processing	Multiple subparts need to be manufactured with minimal post-processing but require joining/welding/riveting	Multiple subparts need to be manufactured with significant post-processing but require joining/welding/riveting	Parts with reasonable size scale cannot be manufactured
	Near Net Shaping (Complexity of Shape)	How complex of a shape can the manufacturing process of a material make?	Not limited by the complexity of the design	Somewhat limited by the complexity of the design	Limited but few complex geometries can be achieved	Only simple geometries can be achieved	Only 1D/2D geometries are possible

4.2 Materials Evaluation with Decision Criteria

This section describes the application results of the decision criteria matrix for the AM ODS alloys. To compensate for the lack of existing properties data and uncertainties in processing, application of the decision criteria matrix has used many possible means, including the data in the known knowledgebase for similar materials or the variants from traditional manufacturing methods, newly produced experimental data, and postulated knowledge from experience.

Table 7 and Table 8 list the decision criteria in four groups that are chosen as materials-evaluation items for downselecting the new materials. The numbers listed in the last two columns are the corresponding scores for the additively manufactured ferritic and austenitic ODS steels, and those given in the middle column are the reasonings for deciding these scores. The scores given to the materials range from 1 to 5, and the detailed criteria matrix used to decide these scores are tabulated in the previous subsection.

Table 7. Application space and environmental compatibility criteria and scores for the ODS materials

Category	Criteria	Reasoning for Scores	Ferritic ODS Steels	Austenitic ODS Steels
Application Space	Applicability to Different Reactor Types	The ferritic or ferritic-martensitic steels are suited for many Gen-IV reactors. For some radioactivation and nuclear transmutation reasons, the austenitic steels are disadvantaged for a few reactor types.	4	3
	Other Industry Experience	Both ferritic and austenitic ODS alloys are new to any industrial applications.	1	1
	Data Availability	Significant data are available for the ferritic ODS alloys, but not for the austenitic alloys.	3	2
	Code & Standards Availability	No availability of codes and standards for production, material qualification, and implementation of any ODS materials.	1	1
	Component Versatility	Potential application of ODS materials may be limited to some function-critical components such as reactor core components.	3	3
Environmental Compatibility	Radiation Resistance	Nanostructured ODS materials have high radiation resistance such as low swelling and relatively lower degradation in mechanical properties.	4	4
	Elemental Transmutation	The ferritic Fe-Cr alloys will show very limited transmutation in irradiation, while some elements (like Ni) in the austenitic Fe-Cr-Ni alloy can be transmutant.	4	3
	High Temperature Oxidation Resistance	Oxidation in the austenitic alloys is highly limited up to 600°C. The oxidation resistance of ferritic alloys is relatively lower.	3	4
	Neutronics Compatibility	Negative impact to the neutron economy is acceptable for both alloy groups but the higher Ni content in austenitic alloys gives some negative impact.	4	3
	Coolant Compatibility & Corrosion Resistance	The ferritic Fe-Cr alloys show corrosion resistance in many coolant environment, while the austenitic Fe-Cr-Ni alloys can provide higher resistance.	3	4

Table 8. Physical and mechanical properties and manufacturability criteria and scores for the ODS materials

Category	Criteria	Evaluation	Ferritic ODS Steels	Austenitic ODS Steels
Physical & Mechanical Properties	Thermal Conductivity	The thermal conductivity of both ferritic and austenitic ODS alloys may be maintained at 10 - 50 W/m.K, although the value of austenitic alloys is near the lower end in irradiation.	3	3
	Thermal Capacity	Most Gen-IV reactors are operated at below $0.5T_M$ (melting point) of the steels (1400 – 1500°C).	4	4
	Tensile Properties	Both alloys can achieve a high strength > 1GPa, while the ferritic ODS alloys lose ductility for the gain in strength.	3	4
	Creep Performance	Creep rate is minimal in these alloys, and no creep rupture is expected in the load and temperature ranges of reactors.	4	4
	Fatigue	Both ODS alloys are high strength materials and the loads in most reactors are well below their fatigue limits.	4	4
	Fracture Toughness	Austenitic ODS alloys may retain high fracture toughness (>100 MPa√m) in most reactor types. However, the fracture toughness of ferritic ODS alloys depends strongly on the manufacturing route.	2	4
	Microstructural Dependency	The properties of both alloys have medium level sensitivity to their microstructures.	3	3
	Scope for Microstructural Enhancement	Microstructure can be easily controlled for desirable properties within advanced processing means. Limitation may exist in mass production.	4	4
Manufacturability	Reproducibility/ Consistency	A high degree of reproducibility and consistency in product quality can be achieved with the AM and post-build TMT route, which is only for small ODS alloy products. The ferritic ODS alloys are more sensitive to the production parameters.	3	4
	Process Complexity	A few post-build processing steps are needed in addition to the conventional manufacturing routes.	3	3
	Cost	The overall cost for additively manufactured ODS alloys is estimated to be higher (10-30%) than the traditional processing methods.	2	2
	Scalability	Both ODS alloys and their manufacturing processes have a good potential for the mass production of small size components, but not for the production of large components.	2	2
	Production Method TRL	Manufacturing processes for both ODS alloys should be with the mid-TRL between 3 and 5. Note that there is some experience in tube (fuel cladding) fabrication.	3	3
	Raw Material Supply	Raw materials are easily available in the United States.	4	4
	Flexibility of Manufacturing	All steps but the AM in the manufacturing routes can be conventional or a combined manufacturing method.	4	4

Table 8 (continued). Physical and mechanical properties and manufacturability criteria and scores for the ODS materials

Category	Criteria	Evaluation	Ferritic ODS Steels	Austenitic ODS Steels
	Conventional Machining	Multiple steps and subparts will be needed for manufacturing of any ODS alloy components. But Little joining may be needed in some austenitic alloy components.	3	4
	Near Net Shaping (Complexity of Shape)	Ferritic ODS steels may be used for only simple geometries such as plate and tube. Much more complex components can be provided with the austenitic ODS alloys for their uniquely high ductility.	2	4

As listed in these two tables, many of the decision criteria are scored the same for the AM ferritic and austenitic ODS alloys. However, the austenitic alloys generally have higher corrosion resistance and significantly better ductility. Furthermore, these two edges in the properties lead to additional favorable decisions or better scores for the austenitic ODS materials. The average scores are 3.07 and 3.26, respectively, for the ferritic ODS alloys and austenitic ODS alloys. Although these scores are not significantly different to make them discernable, the austenitic ODS alloys were selected to be the primary materials group in the future research on ODS materials in the AMMT program.

5. CONCLUDING REMARKS

[1]. The work package aimed to explore the advanced manufacturing techniques that are feasible for the manufacturing of advanced materials components. The main efforts were exerted to identify an accelerated development path for ODS alloys by creatively combining AM technologies with the recent advances in ODS materials and traditional manufacturing technologies. An AM and post-build processing route was developed for ODS ferritic (Fe-Cr alloy or 14YWT) and austenitic (Fe-Cr-Ni alloys or 316L and 316H) alloys. Basic microstructural and mechanical characterizations were performed to provide feedback to the alloy and processing design. Furthermore, multiple laboratories collaborated to create a decision criteria matrix to evaluate and downselect the new materials processed by advanced manufacturing methods.

[2]. New ODS alloy processing routes combining AM processes and post-build TMTs were designed and applied to the production of 15 variants of ferritic and austenitic ODS materials. The AM processes include DED for ferritic alloys and LPBF for austenitic alloys, and the post-build TMTs were 700°C and 800°C controlled hot-rolling steps.

[3]. Key mechanical test results including tensile strength, tensile ductility, and fracture toughness data and are reported and explained. The highest strength among the ODS variants (YS > 1 GPa) was measured from a ferritic ODS alloy, and the highest ductility (TE > 40%) and fracture toughness (K_C > 200 MPa√m) were measured from austenitic ODS alloys.

[4]. Many of the decision criteria were scored the same for the AM ferritic and austenitic ODS alloys; however, the austenitic alloys generally have higher corrosion resistance and significantly better ductility, yielding a slightly higher average score than the ferritic alloys (3.26 vs. 3.07). Therefore, the austenitic ODS alloy was downselected to be the primary materials type in the future research on ODS materials in the AMMT program.

6. REFERENCES

[1] Steven J. Zinkle, Jeremy T. Busby, "Structural materials for fission & fusion energy," *Materials Today,* 12 (2009) 12-19.

[2] Lizhen Tan, Thak Sang Byun, Yutai Katoh, Lance Lewis Snead, "Stability of MX-type strengthening nanoprecipitates in ferritic steels under thermal aging, stress and ion irradiation," *Acta Mater.,* 71 (2014) 11-19.

[3] M.B. Toloczko, D.S. Gelles, F.A. Garner, R.J. Kurtz, K. Abe, "Irradiation creep and swelling from 400 to 600 C of the oxide dispersion strengthened ferritic alloy MA957," *J. Nucl. Mater.,* 212 (1994) 604-607.

[4] Osman Anderoglu, Thak Sang Byun, Mychailo Toloczko, Stuart A Maloy, "Mechanical performance of ferritic martensitic steels for high dose applications in advanced nuclear reactors," *Metall. Mater. Transact.,* A44 (2013) 70-83.

[5] T.S. Byun, J.H. Kim, J.H. Yoon, D.T. Hoelzer, " High Temperature Fracture Characteristics of Nanostructured Ferritic Alloy (NFA)," *J. Nucl. Mater. ,* 407 (2010) 78-82.

[6] T.S. Byun, J.H. Yoon, S.H. Wee, D.T. Hoelzer, S.A. Maloy, ",Fracture Behavior of 9Cr Nanostructured Ferritic Alloy with Improved Fracture Toughness," *J. Nucl. Mater.,* 449 (2014) 39-48.

[7] Thak Sang Byun, Ji Hyun Yoon, David T. Hoelzer, Yong Bok Lee, Suk Hoon Kang, Stuart A Maloy, "Process Development for 9Cr Nanostructured Ferritic Alloy (NFA) with High Fracture Toughness," *J. Nucl. Mater. ,* 449 (2014) 290-299.

[8] D.T. Hoelzer, "History and Outlook of ODS/NFA Ferritic Alloys for Nuclear Applications," *Trans. ANS,* 118 (2018) 1587-1590.

[9] D.T. Hoelzer, J. Bentley, M.A. Sokolov, M.K. Miller, G.R. Odette, M.J. Alinger, "Influence of particle dispersions on the high-temperature strength of ferritic alloys," *J. Nucl. Mater.,* 367–370 (2007) 166-172.

[10] X.L. Wang, C.T. Liu, U. Keiderling, A.D. Stoica, L. Yang, M.K. Miller, C.L. Fu, D. Ma, K. An, "Unusual thermal stability of nano-structured ferritic alloys," *,J. Alloys & Compounds,* 529 (2012) 96-101.

[11] C.P. Massey, D.T. Hoelzer, P.D. Edmondson, A. Kini, B. Gault, K.A. Terrani, S.J. Zinkle, "Stability of a model Fe-14Cr nanostructured ferritic alloy after long-term thermal creep," *Scripta Mater.,* 170 (2019) 134-139.

[12] M. Toloczko, "FCR&D Report," (2014).

[13] K.G. Field, J. Simpson, M. N. Gussev, H. Wang, M. Li, X. Zhang, X. Chen, T. Koyanagi, K. Kane, A. Marquez Rossy, M. Balooch, and K.A. Terrani, "Handbook of Advanced Manufactured Material Properties from TCR Structure Builds at ORNL – FY19," ORNL/TM-2019/1328, Oak Ridge National Laboratory, 2019.

[14] T. S. Byun, M. N. Gussev, T. G. Lach, M. R. McAlister, J. J. Simpson, B. E. Garrison, Y. Yamamoto, C. B. Joslin, J. K. Carver, F. A. List, R. R. Dehoff, K. A. Terrani, M. Li, X. Zhang,

"Mechanical Properties and Deformation Behavior of Additively Manufactured 316L Stainless Steel – FY 2020," ORNL/TM-2020/1574, Oak Rodge Nationalaboratory, 2020.

[15] T.S. Byun, B.E. Garrison, M.R. McAlister, X. Chen, M.N. Gussev, T.G. Lach, A. Le Coq, K. Linton, et al., "Mechanical behavior of additively manufactured and wrought 316L stainless steels before and after neutron irradiation," *J. Nucl. Mater.,* 548 (2021) 152849.

[16] B. M. Morrow, T. J. Lienert, C. M. Knapp, J. O. Sutton, M. J. Brand, R. M. Pacheco, V. Livescu, J. S. Carpenter, G. T. Gray, "Impact of Defects in Powder Feedstock Materials on Microstructure of 304L and 316L Stainless Steel Produced by Additive Manufacturing," *Metall. Mater. Trans. A,* 49 (2018) 3637–3650.

[17] T. Ronneberg, C. M. Davies, and P. A. Hooper, "Revealing Relationships between Porosity, Microstructure and Mechanical Properties of Laser Powder Bed Fusion 316L Stainless Steel through Heat Treatment," *Mater. Des.,* 189 (2020) 108481.

[18] A. J. Birnbaum, J. C. Steuben, E. J. Barrick, A. P. Iliopoulos, J. G. Michopoulos, "Intrinsic Strain Aging, Σ3 Boundaries, and Origins of Cellular Substructure in Additively Manufactured 316L," *Addit. Manuf.,* 29 (2019) 100784.

[19] U. S. Bertoli, B .E. MacDonald, J. M. Schoenung, "Stability of Cellular Microstructure in Laser Powder Bed Fusion of 316L Stainless Steel," *Mater. Sci. Eng. A,* 739 (2019) 109–117.

[20] M. Li, X. Zhang, W.Y. Chen, F. Heidet, T. S. Byun, K.A. Terrani, "Creep Behavior of 316L Stainless Steel Manufactured by Laser Powder Bed Fusion," *J. Nucl. Mater.,* 548 (2021) 152847.

[21] T. Kurzynowski, K. Gruber, W. Stopyra, B. Kuźnicka, E. Chlebus, "Correlation between Process Parameters, Microstructure and Properties of 316 L Stainless Steel Processed by Selective Laser Melting," *Mater. Sci. Eng. A,* 718 (2018) 64–73.

[22] C. R. Brinkman, "Elevated-Temperature Mechanical Properties of an Advanced Type 316 Stainless Steel, United States," ORNL/CP-101053, Oak Ridge National Laboratory, 1999.

[23] E. Garlea, H. Choo, C. C. Sluss, M. R. Koehler, R. L. Bridges, X. Xiao, Y. Ren, B. H. Jared, "Variation of Elastic Mechanical Properties with Texture, Porosity, and Defect Characteristics in Laser Powder Bed Fusion 316L Stainless Steel," *Mater. Sci. Eng. A,* 763 (2019) 138032.

[24] T. Pinomaa, M. Lindroos, M. Walbrühl, N. Provatas, A. Laukkanen, "The Significance of Spatial Length Scales and Solute Segregation in Strengthening Rapid Solidification Microstructures of 316L Stainless Steel," *Acta Mater.,* 184 (2020) 1–16.

[25] D. Kong, X. Ni, C. Dong, L. Zhang, C. Man, X. Cheng, and X. Li, "Anisotropy in the Microstructure and Mechanical Property for the Bulk and Porous 316L Stainless Steel Fabricated via Selective Laser Melting," *Mater. Lett. ,* 235 (2019) 1–5.

[26] J. Lin, F. Chen, X. Tang, J. Liu, S. Shen, and G. Ge, "Radiation-Induced Swelling and Hardening of 316L Stainless Steel Fabricated by Selected Laser Melting," *Vacuum,* 174 (2020) 109183.

[27] M. Song, M. Wang, X. Lou, R. B. Rebak, and G. S. Was, "Radiation Damage and Irradiation-Assisted Stress Corrosion Cracking of Additively Manufactured 316L Stainless Steels," *J. Nucl. Mater.,* 513 (2019) 33–44.

[28] G. Meric de Bellefon, K.M. Bertsch, M.R. Chancey, Y.Q. Wang, D.J. Thoma, "Influence of solidification structures on radiation-induced swelling in an additively-manufactured austenitic stainless steel," *J. Nucl. Mater.,* 523 (2019) 291-298.

[29] N. Sridharan, M.N. Gussev, K.G. Field,, "Performance of a ferritic/martensitic steel for nuclear reactor applications fabricated using additive manufacturing,," *J. Nucl. Mater.,* 521 (2019) 45-55.

[30] W. Zhong, N. Sridharan, D. Isheim, K.G. Field, Y. Yang, K. Terrani, L. Tan,, "Microstructures and mechanical properties of a modified 9Cr ferritic-martensitic steel in the as-built condition after additive manufacturing," *J. Nucl. Mater.,* 545 (2021) 152742.

[31] T.S. Byun, S.A. Maloy and J.H. Yoon, "Small Specimen Reuse Technique to Evaluate Fracture Toughness of High Dose HT9 Steel," *Small Specimen Test Tech., ASTM International* , STP-1576 (2015) 121-141.

[32] T. Hartmann, S. Maloy, M. Komarasamy, "Materials Scorecards, Phase 2," March 2022.